Journal of Applied Polymer Science

Interface Self-Reinforcing Ability and Antibacterial Effect of Natural Chitosan Modified Polyvinyl Chloride-Based Wood Flour Composites

Kaimeng Xu,[1] Kaifu Li,[1] Tuhua Zhong,[2] Chengping Xie[3]

[1]Department of Forestry, South China Agricultural University, Guangzhou 510642, People's Republic of China
[2]Division of Forestry and Natural Resources, West Virginia University, Morgantown, West Virginia 26505
[3]China Electronic Product Reliability and Environmental Testing Research Institute, Guangzhou 510610, People's Republic of China
Correspondence to: K. M. Xu (E-mail: xukm007@163.com) or K. F. Li (E-mail: kfli@scau.edu.cn)

ABSTRACT: Natural chitosan (CS) at four different additions (10, 20, 30, and 40 phr) and particle size ranges (100–140, 140–180, 180–220, and over 260 mesh) are selected to improve the interface adhesion as well as endow a novel antibacterial function to wood flour/polyvinyl chloride (WF/PVC) composites. In the present study, we investigate the interface self-reinforcing ability of CS to composites by Fourier transform infrared spectroscopy (FTIR), scanning electron microscopy (SEM), dynamic mechanical analysis (DMA), mechanical testing instrument, and water absorption behavior test (WB). The antibacterial activity is also estimated by the method of membrane covering test (MCT) using *Escherichia coli*. The results recorded show that adding 30 phr CS with the particle size of over 260 mesh is considered to be perfect selection to prepare the excellent interfacial self-reinforcing and antibacterial WF/PVC/CS composites. © 2013 Wiley Periodicals, Inc. J. Appl. Polym. Sci. **2014**, *131*, 39854.

KEYWORDS: surfaces and interfaces; biopolymers and renewable polymers; compatibilization; morphology; poly(vinyl chloride)

Received 4 June 2013; accepted 15 August 2013
DOI: 10.1002/app.39854

INTRODUCTION

Due to the worsening shortage crisis of natural resources and energy in recent years, high-valued utilizations of agricultural and forestry biomass to develop emerging materials have been springing up in diverse fields to effectively relieve the pressure of ecology and sustainable development. Also of great concern is the use of wood plastic composites (WPC) as one of most potential novel materials. The polymer matrix which includes polyethylene (PE), polypropylene (PP), and polyvinyl chloride (PVC), and biomass fiber such as wood, bamboo, kenaf, hemp, sisal and other agricultural residuals are two major components used in WPC manufacturing.[1–5] There was a considerable growth rate of 200% from 2002 to 2010 for PVC-based wood flour composites owing to its unique decoration, paintable surface, high stiffness, creep resistance, durability, and natural flame retardant quality compared to PP- and PE-based WPC.[6,7] Therefore, they were employed to partially substitute solid wood or wood-based boards in building constructions and decoration applications.[8,9]

However, it is the interface problem between hydrophilic biomass fiber and hydrophobic polymers that impeded the improvement of mechanical performance for WPC.[10] The latest published information about mechanical strength improvement of PVC-based wood flour composites mainly focused on the reinforcing approaches such as the additions of chemical compatilizers and modifiers,[11–13] glass-fiber,[14,15] carbon nanotubes,[16] and nanoparticles[3,17] as well as surface adhesion using high carbon steel flat bar strips.[18,19] Unlike the C—C and C—H bonds in PP and PE molecular chains, there were additional C—Cl bonds in PVC molecular chains, which led to the special interface situation for PVC-based wood flour composites. Typical theory has pointed out that a significant factor to the effective interfacial adhesion between PVC and biomass fiber is acid–base interactions, in which one phase acts as base-donating electrons and the other acts as acid-accepting electrons.[20–22] According to the relevant theory and previous publications, it can be noticed that there may be several disadvantages for those enhancing methods mentioned above. Generally, they were expensive, complicated technology processes and poor dispersion in composites.

Chitosan (CS), which is the second most abundant natural polymer closely following cellulose, is extracted from crustaceous shells of ocean biomasses such as crabs, shrimps, and prawns. It is well known to possess huge quantities, nontoxicity, biodegradability, biocompatibility, low cost as well as excellent mechanical, thermal, and antibacterial properties.[23–26] Recent

studies stated that CS and its modifying products were useful reinforcing agents for elevating the mechanical strength of polymeric composite materials.[27–30] Shah et al.[31] directly filled chitin and CS into formulations to produce PVC-based wood flour composites by the method of mold pressing. They found that the flexural strength and modulus of composites performed greater than the unfilled composites and neat PVC. The optimum addition amount of chitin and CS was 6.67 and 0.5 wt %, respectively. In our previous study,[32] CS dissolved into diluted acetic acid was added into formulations, and two-steps connecting extrusion technology was adopted to prepare better dispersing PVC-based wood flour composites. The thermal and rheological properties with and without CS were investigated. The results indicated that CS can provide positive effects on heat resistance and thermal stability at early stage of degradation but a little negative effect on rheological characteristic. Improvement of interface adhesion also can be verified indirectly by the thermal analyses.

Antibacterial activity was another feature for CS. Based on this, CS currently has been widely utilized to produce biomedical membrane, food packaging materials, and other novel nanocomposites.[33–36] Nevertheless, up to now, there was no study on its antibacterial function for the utilization of WPC. In order to expand the applications of WPC further, it is essential to develop some functional WPC with the specific properties such as antibacterium, mold proofing, static resistance, and so on.

In our present work, we prepared the wood flour/PVC/CS composites by the "two-step" method that mocked practical production by connecting the counter-rotating twin-screw extrusion with conical twin-screw extrusion. We mainly aimed at investigating the self-reinforcing ability of excellent interface adhesion after adding CS with various contents and particle sizes as well as its natural antibacterial effects to PVC-based wood flour composites. The interfacial self-reinforcing ability was characterized and analyzed by using Fourier transform infrared spectroscopy (FTIR), scanning electron microscopy (SEM), and dynamic mechanical analysis (DMA). Meanwhile, mechanical properties (flexural and tensile strengths) tests and water absorption behavior test (WB) were employed to indirectly confirm the improvement as well. *Escherichia coli* were first used to evaluate the natural antibacterial activity for WPC without any chemical antibacterial agents.

EXPERIMENTAL

Materials

PVC (DG-800, *K* value-62) with the average degree of polymerization of 800, density 1.35–1.45 g/cm^3 was supplied by Tianjin Dagu Chemical, China. Wood flour (*Cunninghamia lanceolata*) with a size distribution of 150–180 μm was obtained from Guangzhou Minshan New Material, China. The flakes of CS with the degree of deacetylation and an average molecular mass of 95% and 820,000 respectively, were purchased from Goldenshell Biochemical, China. To complete the formulation, the other additives including chlorinated PE, acrylamide, calcium zinc stabilizer, diethylhexyl phthalate, glycerin monostearate, and paraffin wax were bought from local chemical companies.

Table I. Main Formulation for WF/PVC Composites

Groups	WF (phr)	CS (phr)	Size distribution of CS (mesh)
WF/PVC	40	0	0
WF/PVC/CS-10	40	10	80–100
WF/PVC/CS-20	40	20	80–100
WF/PVC/CS-30	40	30	80–100
WF/PVC/CS-40	40	40	80–100
WF/PVC/CS-a	40	25	100–140
WF/PVC/CS-b	40	25	140–180
WF/PVC/CS-c	40	25	180–220
WF/PVC/CS-d	40	25	>260

E. coli (ATCC 8739) were provided by Guangdong Institute of Microbiology, China.

Composites Preparation

The flakes of CS were smashed in a high-speed disintegrator, then sieved to required particle size using the vibrating screen equipping with the sieves of specific mesh number. The prepared CS were added into 2 wt % acetic acid solution with stirring at 40°C for 30 min. Afterward, the solution was cooled down to room temperature, then stored in a sealed container for use.

WF was dried at 105 ± 2°C for 48 h in an oven to make sure the moisture content less than 1%. WF and PVC were premixed in a high-speed mixer (SHR-10A, Zhangjiagang, China) with 1600 rpm at 80°C for 5 min. The diluted solution of CS was sprayed into the compound system to blend for 15 min at a main formulation (Table I). Other additives including plasticizer (6 phr), heat stabilizer (5 phr), lubricant (1 phr), and modifier (6 phr) were also added and mixed at 105°C for 10 min.

Subsequently, the blending was extruded as a shape of rod by counter-rotating twin-screw extruder (SHJ-20, Nanjing, China) in the temperature range of 150–180°C with the average rotation speed of 10 rpm. After cooling down by water, the extrudate was pelleted using a granulator and dried at 80 °C by blowing. Finally, the granules were transferred to a conical twin-screw extruder (LSE-35, Guangzhou, China) to produce sheet samples. The processing temperature during extrusion was set at the range of 125–185°C from hopper to die zone. The rotation speed of twin screw was 30 rpm with the 12 rpm for single screw. Afterward, all the sheets were cut into required dimensions for further tests in accordance with the related standards.

Interface Self-Reinforcing Ability Analysis

The microinterfacial morphology and the ability of interfacial self-reinforcing improvement of CS to WF/PVC composites were studied by FTIR, SEM, and DMA.

FTIR analysis of the WF/PVC/CS composites was performed using a Tensor 27 (Bruker, Germany) at ambient temperature to investigate the interfacial bonding enhancement due to adding the natural CS. Each spectrum was recorded at a resolution of

2 cm^{-1} with a total 64 scans in the wave number range of 4000–400 cm^{-1}.

The observation of microinterfacial morphology of WF/PVC/CS composites was carried out on a SEM (Hitachi S-3400, Philips, Japan) with an accelerating voltage of 10 kV. The specimens were frozen in liquid nitrogen, fractured, dried, and sputter-coated with a thin layer of gold before observation.

The DMA (242C, Netzsch, Germany) was employed to study the storage modulus (E') and mechanical damping factor ($\tan\delta$) of WF/PVC/CS composites in the three point bending mode. The specimen size for the test was 55 mm (length) × 11 mm (width) × 4.8 mm (thickness). DMA scans were recorded at frequency of 1 Hz in the temperature range of 25–150°C with a heating rate of 3°C/min.

Water Absorption Behavior Test

The water-absorption behavior test was conducted following a modified procedure originally described in ASTM D570-95. Five replicate specimens with dimensions of 20 × 20 × 5 mm^3 (thickness) were completely immersed into water at 23 ± 2°C for 48 days. The weight changes were measured every 2 days. Each sample was dried using tissues before measuring to remove excess water, immediately weighed, and then immersed again in the water for next measurement. The rate of water absorption was calculated based on the weight percent changes.

The water absorption behavior for the composites after adding different contents and particle sizes CS can also be studied using eq. (1).[37,38]

$$\frac{M_t}{M_\infty} = 4\left(\frac{Dt}{\pi h^2}\right)^{\frac{1}{2}} \quad (1)$$

where M_t is the moisture content at certain time, M_∞ is the maximum moisture content measured at the end of the test. D is the diffusion coefficient and h is the sample thickness corresponding to M_∞. Hence, the diffusivity D can be calculated by the slope of the moisture absorption versus the square root of time.

Mechanical Properties Measurements

Flexural specimens with a dimension of 110 mm × 20 mm × 5.5 mm (thickness) were measured by using mechanical instrument (CMT5504, Shenzhen, China) according to ASTM D790-2004, which involved a three-point bending test. The speed of crosshead and span length was 2 mm/min and 88 mm, respectively. The tensile tests were carried out according to ASTM D 638-2004 at a speed of 2 mm/min. The size of the samples was 165 × 20 × 5.5 mm^3 (thickness). Five replicate specimens were tested for standard deviations.

Antibacterial Property Measurements

The antibacterial performances of samples were evaluated by membrane covering test (MCT).[39] *E. coli* (ATCC 8739) were selected as the indicators in antibacterial experiment. The microorganisms of *E. coli* were grown in the medium of nutrient agar (NA) broth at 37 ± 1°C for 24 h under the condition of oxygen. Next steps were all operated on the clean bench.

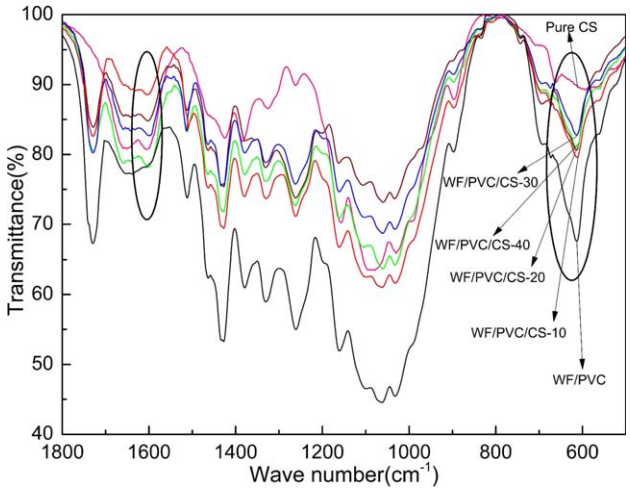

Figure 1. FTIR spectra of samples with different contents CS. [Color figure can be viewed in the online issue, which is available at wileyonlinelibrary.com.]

Each specimen with the dimension of 30 × 30 × 5 mm^3 (thickness) was washed and sterilized using sterilized water, 95% ethanol for 10 min, and then dried in a clean cabinet. The fresh cultivated *E. coli* was scraped down from NA broth and diluted to the suitable concentration. Subsequently the solution was dropping on the samples with the PE thin membrane covering in the Petri dish. Finally, all specimens were incubated at the temperature of 37 ± 1°C, relative humidity of 95 ± 2% for 24 h. The bacteria on the specimens were collected and spread onto an NA plate to culture at 37 ± 1°C for 24 h.

The evaluation of MCT was determined by contrasting the recoded numbers of bacterial colonies for different groups. The lower numbers of bacterial colonies showed the better antibacterial activity for composites. The antibacterial rate (AR) was calculated as follows:

$$\mathrm{AR} = \frac{C_2 - C_1}{C_2} \times 100\% \quad (2)$$

where AR is the antibacterial rate, C_2 and C_1 are the numbers of bacterial colonies of samples without CS and the samples with different contents and particle sizes CS, respectively.

RESULTS AND DISCUSSION

Interface Self-Reinforcing Ability Analysis

FITR Analysis. The FTIR spectra and data of pure CS and WF/PVC/CS with different addition amounts of CS (0–40 phr) can be observed in Figure 1 and Table II. There were three key bands in the wave number regions of 600–700, 1601–1604, and 3416–3442 cm^{-1} corresponding to the carbon–chlorine (C—Cl) stretching vibration, amino (NH) groups bending vibration, as well as hydroxyl (OH) and amino (NH) groups stretching vibrations, respectively, which were closely related to the interfacial reinforcement ability. The 693.95 cm^{-1} band was assigned to C—Cl stretching vibration with "I" configuration and "TGTG" conformation in PVC chains. The 673 and 613 cm^{-1} band correspond to the C—Cl stretching vibration with "S" configuration and the conformations of "TTGG" as well as "TT

Table II. Variation Situations of Three Key Bands of C-Cl, NH, and OH Vibrations for Different Groups Composites

Groups	Wave number of C-Cl (cm^{-1})	Transmittance of C-Cl(%)	Wave number of OH and NH (cm^{-1})	Transmittance of OH and NH (%)
Pure CS	None	None	3442.35, 1603.96	63.25, 80.75
WF/PVC	693.95, 613.94	79.53, 67.57	3419.40, None	73.30, None
WF/PVC/CS-10	673.90, 613.82	86.99, 79.57	3417.34, 1601.83	67.75, 88.54
WF/PVC/CS-20	673.42, 613.25	88.11, 80.59	3417.32, 1601.71	64.60, 84.79
WF/PVC/CS-30	672.59, 612.76	90.14, 82.75	3416.71, 1600.89	61.25, 82.70
WF/PVC/CS-40	672.94, 613.44	88.12, 80.88	3417.17, 1601.57	41.92, 78.14
WF/PVC/CS-a	674.87, 613.96	83.46, 73.87	3423.88, 1601.85	72.34, 85.72
WF/PVC/CS-b	673.39, 613.75	85.47, 76.55	3417.45, 1601.48	68.19, 85.48
WF/PVC/CS-c	672.51, 613.69	87.83, 80.04	3417.18, 1601.27	66.31, 85.11
WF/PVC/CS-d	671.18, 612.05	90.64, 85.07	3417.17, 1601.14	64.67, 84.19

short trans sequences," respectively.[40] In combination with the data in Table II, it was significant to note that the wave number of 693.95 cm^{-1} dropped noticeably while transmittance increasing after adding the CS for WF/PVC composites. The specific value of wave band of 673 cm^{-1} first decreased from 673.90 to 672.59 cm^{-1} corresponding to the increase of transmittance from 86.99 to 90.14% when CS was added from 10 to 30 phr, whereas over 30 phr followed by a little increase and decrease to 672.94 cm^{-1} and 88.12%. The same variation trend was observed for 613 cm^{-1} band. The lower wave number and higher transmittance indicated that the bonding forces for C—Cl bonds themselves were weaker, which meant both C and Cl atoms had a stronger attraction and adhesion with other ambient atoms. Additionally, the transmittances of hydroxyl (OH) and amino (NH) groups were both declined with the more CS being added. The similar variation trends for their wave number (first reduced to the lowest values, then went back a little) also can be seen in Table II. The lowest wave number values (3416.71 and 1600.89 cm^{-1}) demonstrated that there were the strongest bonding forces existing among NH, OH, and other atoms around at 30 phr CS addition level. The above analyses were expected with the self-reinforcing ability that amine-containing natural CS led to the modified wood surface and the facilitated interaction between wood fiber and PVC matrix in accordance with Lewis acid-base theory.[31]

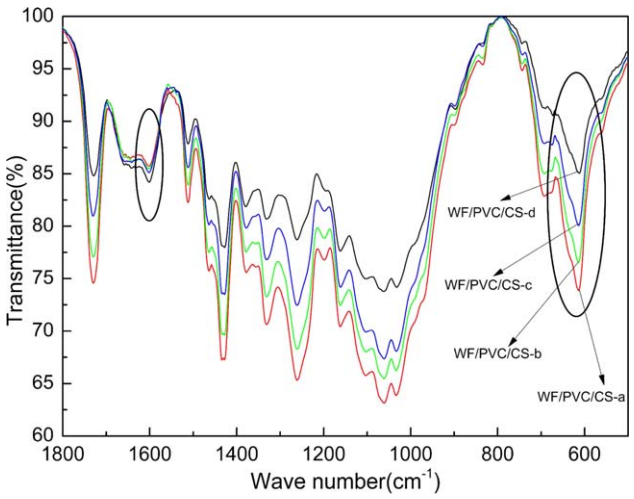

Figure 2. FTIR spectra of samples with different mesh numbers CS. [Color figure can be viewed in the online issue, which is available at wileyonlinelibrary.com.]

Similarly, it can be seen from Figure 2 with specific data in Table II that the interfacial bonding of composites were affected by the various particle sizes of CS at the same addition level of 25 phr. The shifts in the wave number ranges of C—Cl, hydroxyl (OH), and amino (NH) groups went toward lower values as the mesh number increased from the range of 100–140 mesh to over 260 mesh. These implied that the higher mesh number (smaller particle size) could provide a more positive effect on promoting interfacial adhesion as mentioned analysis. Besides, the reason why the transmittances of hydroxyl (OH) and amino (NH) groups decreased with mesh number increasing was attributed to the relatively more CS particles engendering at the larger mesh number level.

SEM Analysis. The morphologic changes of fractured samples with the added CS can be clearly seen from the SEM images shown in Figure 3. The fractured surface of WF/PVC composites without CS was shown in Figure 3(a). The image exhibited some appearances of voids and separated structures, which may be attributed to the pulling out of the wood fiber during fracturing, demonstrating the weak interfacial attachment between wood fiber and PVC matrix. Figure 3(b) shows that the poor interfacial situation turned to better when adding 10 phr CS with a result of decreasing voids. As seen in Figure 3(c,d), the co-continuous phase structures were formed on further addition. There was no extremely obvious difference in the interfacial bonding on increasing the amount of CS from 20 to 30 phr. However, the interface began to appear rough and there was an increasing appearance of voids with the addition amount of CS at 40 phr [Figure 3(e)]. This may be attributed to the partial agglomeration of excess CS. In contrast to the composites without CS, the presence of natural amine groups in CS molecular chains seemed to have favored the interaction

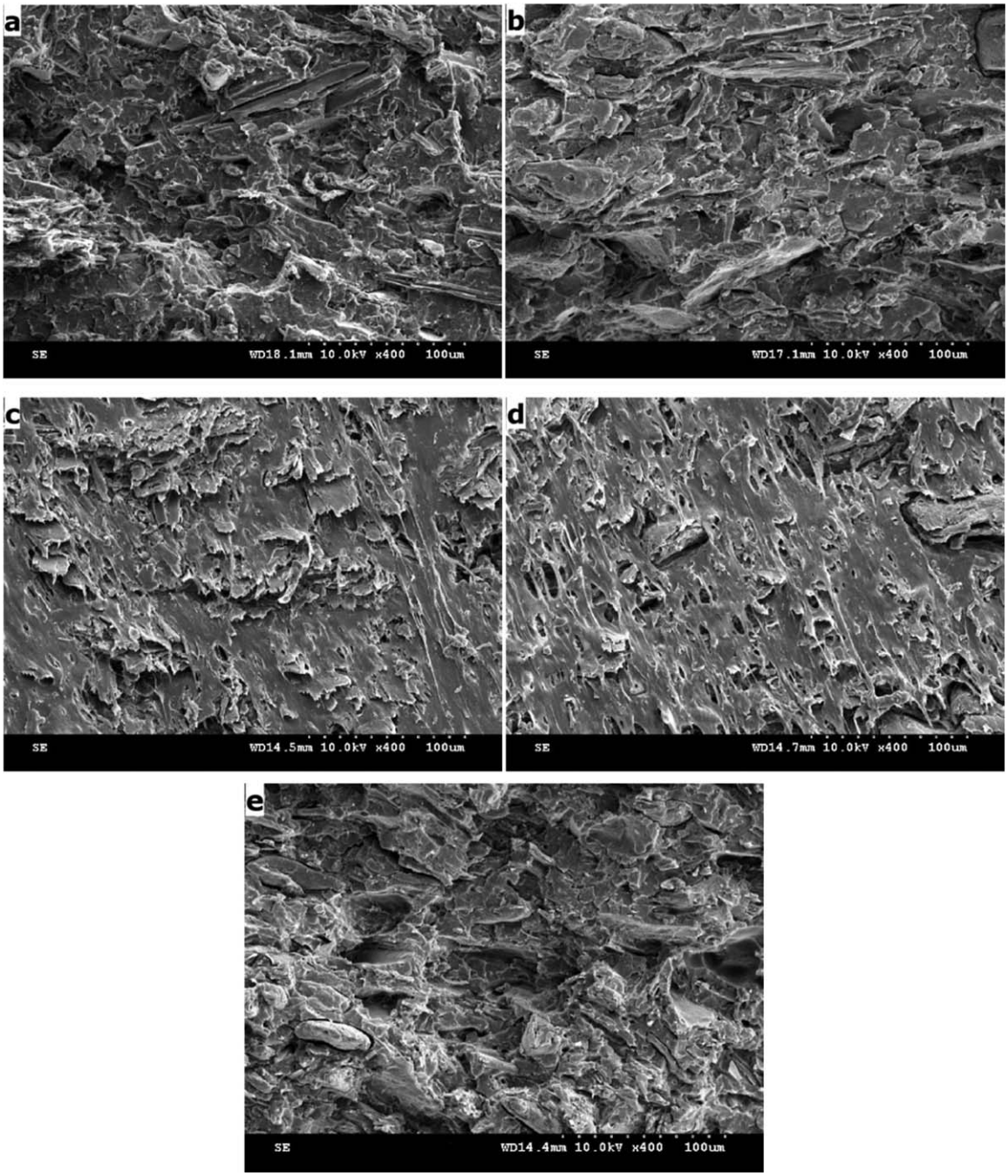

Figure 3. SEM images of samples (a) WF/PVC, (b) WF/PVC/CS-10, (c) WF/PVC/CS-20, (d) WF/PVC/CS-30, and (e) WF/PVC/CS-40.

between PVC matrix and wood fiber based on the analysis mentioned above, which led to a better compatibility between the polymers and wood fiber with CS modification.

We can also observe the effect of different particle sizes on the interface bonding ability from Figure 4 at the same addition amount of CS. The images [Figure 4(a–d)] clearly exhibited that the larger mesh number (smaller particle size) of CS increasing from 100 to over 260 mesh contributed to a less-void and more smooth interface. Similarly, the observed changes of morphology implied that the larger specific surface corresponding to larger mesh number (smaller particle size) has a more effective junction on the interface of wood fiber and PVC matrix.

DMA Analysis. DMA analysis as another method that can reveal the ability of interfacial adhesion enhancement was carried out in the three-point bending model with the temperature range from 30 to 150°C. The results of storage modulus (E')

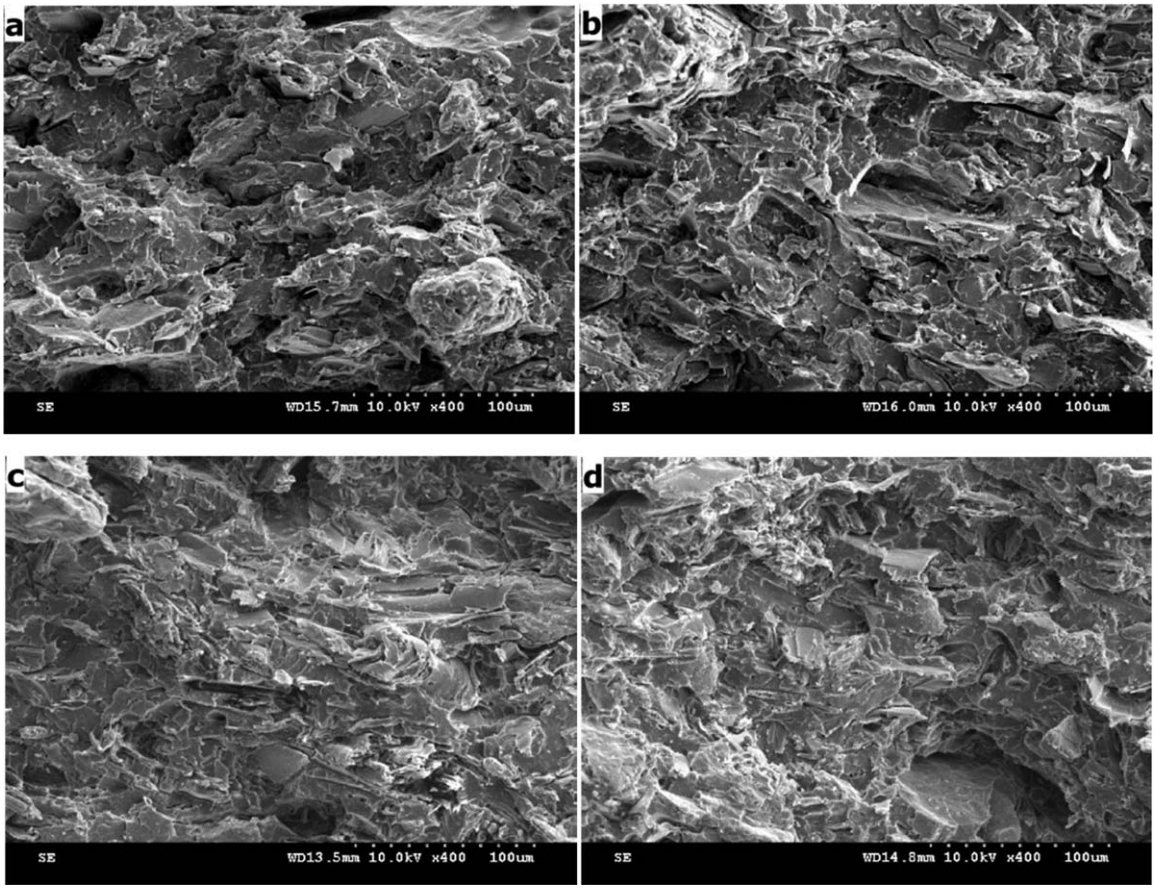

Figure 4. SEM images of samples (a) WF/PVC/CS-a, (b) WF/PVC/CS-b, (c) WF/PVC/CS-c, and (d) WF/PVC/CS-d.

and mechanical damping factor (tanδ) with added different contents and particle sizes CS were shown in Figures 5 and 6.

As seen from Figure 5, all samples for different groups displayed a remarkable elevated E' value from originally 3858–3910, 4341, 5026, and 4463 MPa with respect to CS addition of 0, 10, 20, 30, and 40 phr at 30°C. Meanwhile, it was worth noting that the maximum E' value was obtained when the addition amount was 30 phr. This observation demonstrated that adding CS to WF/PVC compound systems could increase the stiffness owing to inherently wonderful mechanical characteristic of CS as well as self-reinforcing effect incorporated that can transfer a great deal of stress to PVC matrix through the interface.[41] Moreover, an optimum addition (30 phr) promoted the interfacial bonding perfectly. Mechanical damping factor (tanδ) reflected the

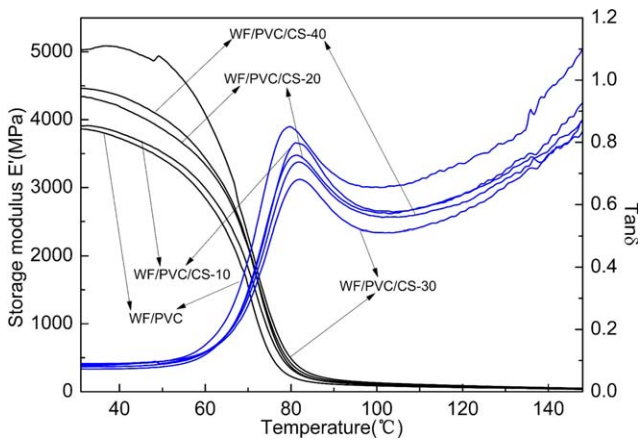

Figure 5. DMA curves for the samples with different contents CS. [Color figure can be viewed in the online issue, which is available at wileyonlinelibrary.com.]

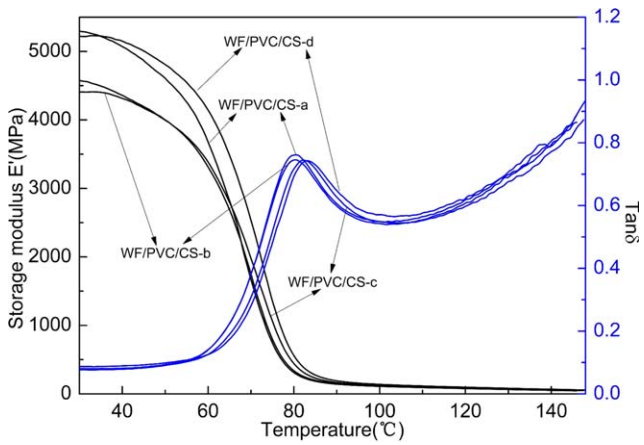

Figure 6. DMA curves for the samples with different mesh numbers CS. [Color figure can be viewed in the online issue, which is available at wileyonlinelibrary.com.]

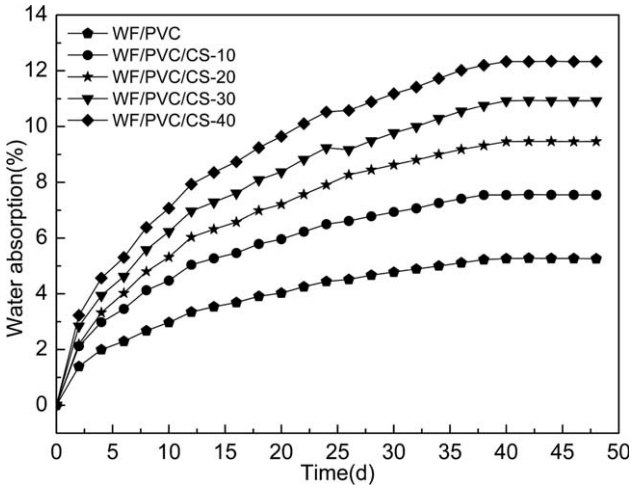

Figure 7. Water absorption curves for the samples with different contents CS.

movement of molecular segments. It was evident from Figure 5 that there was an obvious descend tendency in the peak value of tanδ with addition amount of CS increasing, and it was similar that tanδ value reduced to the minimum value 0.681 from 0.851 at 30 phr. This reason could be explained that stress energy dissipation occurred in the PVC matrix, the stronger interface adhesion drove to dissipate more stress energy well.[42,43] In addition, it was also found that the glass transition temperature (T_g) was prolonged to a higher value after adding CS, which was due to that the effect of CS reinforcement limited the movement of the PVC molecular segments.

Except for selecting proper addition amount of CS for the most effective reinforcing interface characteristic of composites, particle size was indicated to play another significant role for obtaining the excellent bonding performance (Figure 6). The conclusion can be drawn that the relative higher or lower mesh number of CS apparently performed a higher E' than the mesh number at the middle level. The lower value of tanδ for composites was displayed with the mesh number increasing, which suggested that the higher mesh number was preferred in elevating interface compatibility. This was consistent with the analyses mentioned above.

Analysis of Water Absorption Behavior

The results of water absorption of WF/PVC composites with additional 0–40 phr CS were shown in Figure 7 and Table III. Water absorption of composites continuously increased with the prolongation of immersing time for all groups. Typical curves of Fickian diffusion behavior were illustrated as well. The water absorption rate showed rapid linear increase in the initial exposure. Afterward, it slowed down and reached a plateau (pseudo-equilibrium).[44,45] Maximum moisture contents (M_∞) were observed to present an ascending tendency when adding more CS. Although the interfacial adhesion was effectively improved through above analysis, there were more hydrophilic hydroxyl groups in the CS structure embedded into the compound systems during process, which attracted more water molecules resulting in the higher water absorption. On the other hand, there was a basically similar change to diffusion coefficient (D)

Table III. Maximum Water Absorption and Diffusion Coefficient of Composites

Groups	M_∞ (%)	D (mm^2/day)
WF/PVC	5.26	0.689
WF/PVC/CS-10	7.55	0.803
WF/PVC/CS-20	9.47	0.704
WF/PVC/CS-30	10.92	0.762
WF/PVC/CS-40	12.33	0.819
WF/PVC/CS-a	10.72	0.787
WF/PVC/CS-b	9.49	0.777
WF/PVC/CS-c	9.25	0.772
WF/PVC/CS-d	8.88	0.749

with the exception of group WF/PVC/CS-10. A possible explanation was that a relatively low content CS did not play a part in enhancing interfacial bonding well. On the contrary, the hydrophilic hydroxyl groups were brought in leading to a higher diffusion coefficient.

As for the aspect of particle size (Figure 8), there was a relatively great difference for absorption curve and diffusion coefficient of WF/PVC/CS-a at the mesh number range of 100–140 compared to the other three groups. The larger mesh number (smaller particle size) exhibited a stronger water resistance. Nevertheless, the increasing degree for water resistance gradually declined after the mesh number exceeded 180 mesh. The conclusion can be made that an optimum particle size range at the same addition level can provide the most effective improvement to interfacial adhesion and water resistance.

Mechanical Properties Analysis

The mechanical properties (flexural and tensile strength) of WF/PVC composites modified with CS were plotted in Figure 9. The slight reduction for flexural and tensile strengths took place in the WF/PVC composites initially added with 10 phr CS, after that, the flexural and tensile strengths increased with the

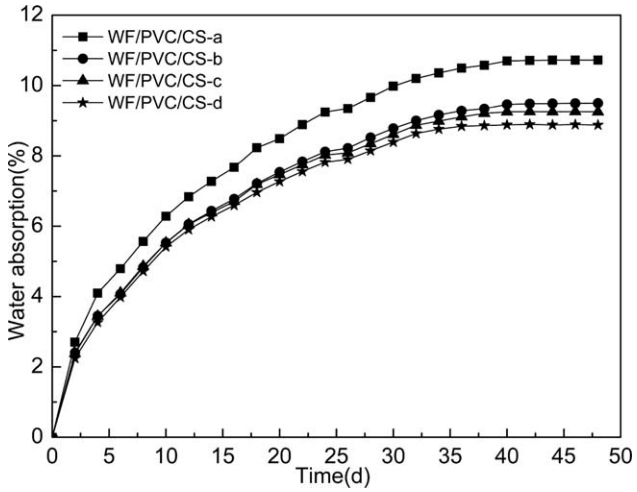

Figure 8. Water absorption curves for the samples with different mesh numbers CS.

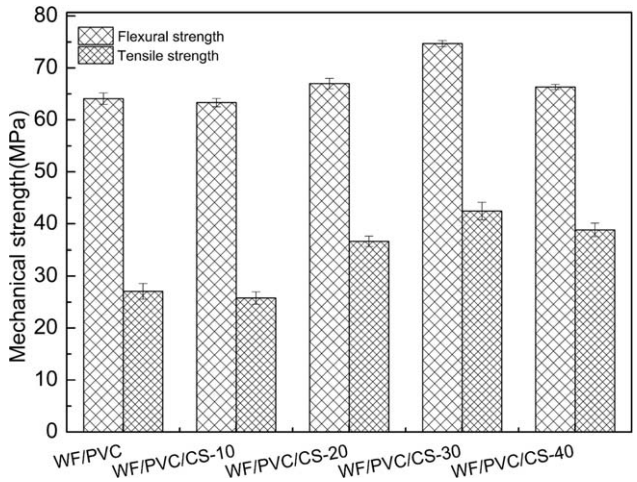

Figure 9. Mechanical strengths of samples with different contents CS.

addition amount of CS increasing. The maximum values 74.7 and 42.45 MPa for both strengths were achieved corresponding to adding 30 phr CS, however, the decline clearly occurred again after exceeding 30 phr. The particle size of CS also had an obvious influence on the mechanical properties of the composites (Figure 10). The composite prepared by larger mesh number (smaller particle size) of CS showed the higher flexural strength value. However, a discrepancy was found for tensile strength. The tensile strength decreased from peak value when the mesh number passed 220 mesh. The above analyses could be used to explain the mechanical performance, but the declining tensile strength was probably explained by the standard deviation.

Antibacterial Property Analysis

Table IV shows the antibacterial results of composites for different addition amounts and particle sizes of CS. It is clearly observed that the lower numbers of bacterial colonies with higher AR is clearly present with the increasing CS content but almost the same level regardless of whether the particle size changed. The maximum for AR was 87.460% corresponding to 40 phr CS. We also noticed that the difference of AR became small after the amount addition surpassing 30 phr, which was

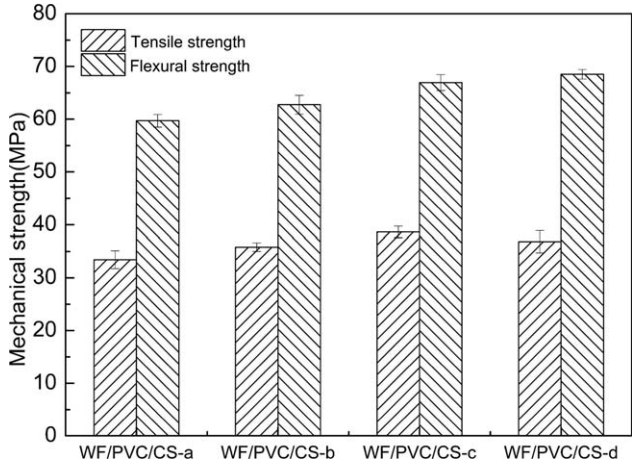

Figure 10. Mechanical strengths of samples with different mesh numbers CS.

Table IV. Antibacterial Results of Different Groups Composites

Groups	AR (%)	Number of bacteria colonies
WF/PVC	0.000	1563
WF/PVC/CS-10	17.594	1288
WF/PVC/CS-20	66.795	519
WF/PVC/CS-30	83.749	254
WF/PVC/CS-40	87.460	196
WF/PVC/CS-a	63.404	572
WF/PVC/CS-b	62.188	591
WF/PVC/CS-c	63.596	569
WF/PVC/CS-d	65.451	520

only 3.711%. The maximum difference of different particle size for AR was 3.263%. Therefore, comprehensively considering mechanical strengths, antibacterial effect, and price cost, adding 30 phr CS with particle size of 260 mesh was perfect selection to prepare outstanding antibacterial and interfacial self-reinforcing WF/PVC composites.

CONCLUSIONS

This study highlighted the interface self-reinforcement ability and antibacterial effect of PVC-based wood flour composites modified by natural CS. The ability for interface self-reinforcement of CS was effectively revealed by the analyses of FTIR, SEM, and DMA. FTIR analysis demonstrated that the addition of CS led to a decrease for the wave number of C—Cl stretching vibration but an increase for their transmittance values, which resulted in a weaker bonding force for C—Cl bonds themselves while a stronger attraction and adhesion with other ambient atoms. SEM images also clearly depicted the variation of interface morphology. Two key characteristic parameters (E' and tanδ) from DMA demonstrated that the more stress energy dissipation and glass transition temperature (T_g) delay occurred after adding CS. Exposure to moisture for long term resulted in obvious increase in water absorption. In addition, antibacterial activity performed well when adding the sufficient CS. In this study, adding 30 phr CS with the particle size of over 260 mesh was considered to be perfect selection to prepare the excellent interfacial self-reinforcing and antibacterial WF/PVC/CS composites.

ACKNOWLEDGMENTS

The authors gratefully acknowledged the financial supports by the grants of the Forestry Scientific and Technological Innovation Funds of Guangdong Province (No. 2011KJCX015-01) and Science and Technology Plan Project Funds of Guangdong Province (No. 2011B020310002).

REFERENCES

1. Wei, L. Q.; McDonald, A. G.; Freitag, C.; Morrell, J. J. *Polym. Degrad. Stab.* **2013**, *98*, 1348.
2. Panthapulakkal, S.; Zereshkian, A.; Sain, M. *Bioresour. Technol.* **2006**, *97*, 265.

3. Deka, B. K.; Maji, T. K. *Compos. A* **2011**, *42*, 686.
4. Najafi, S. K.; Tajvidi, M.; Hamidina, E. *Holz. Roh. Werkst.* **2007**, *65*, 377.
5. Ashori, A. *Bioresour. Technol.* **2008**, *99*, 4661.
6. Fang, Y. Q.; Wang, Q. W.; Bai, X. Y.; Wang, W. H. *J. Therm. Anal. Calorim.* **2012**, *109*, 1577.
7. Jiang, H. H.; Kamdem, D. P. *J. Vinyl Addit. Technol.* **2004**, *10*, 59.
8. Fang, Y. Q.; Wang, Q. W.; Guo, C. G.; Song, Y. M.; Cooper, P. A. *J. Anal. Appl. Pyrol.* **2013**, *100*, 230.
9. Smith, P. M.; Wolcott, M. P. *Forest. Prod. J.* **2006**, *56*, 4.
10. Michaud, F.; Riedl, B.; Castera, P. *Holz. Roh. Werkst.* **2005**, *63*, 380.
11. Jiang, H. H.; Kamdem, D. P. *Appl. Surf. Sci.* **2010**, *256*, 4559.
12. Yue, X. P.; Chen, F.; Zhou, X. S. *Bioresources* **2011**, *6*, 2022.
13. Muller, M.; Gruneberg, T.; Militz, H.; Krause, A. *J. Appl. Polym. Sci.* **2012**, *124*, 4542.
14. Tungjitpornkull, S.; Chaochanchaikul, K.; Sombatsompop, N. *J. Thermo. Compos. Mater.* **2007**, *20*, 535.
15. Tungjitpornkull, S.; Sombatsompop, N. *J. Mater. Process. Technol.* **2009**, *209*, 3079.
16. Farak, O.; Matuana, L. M. *J. Vinyl Addit. Technol.* **2008**, *14*, 60.
17. Deka, B. K.; Maji, T. K. *Compos. Sci. Technol.* **2010**, *70*, 1755.
18. Pulngern, T.; Padyenchean, C.; Rosarpitak, V.; Prapruit, W.; Sombatsompop, N. *Mater. Des.* **2011**, *32*, 3431.
19. Pulngern, T.; Chimkhlai, A.; Rosarpitak, V.; Sombatsompop, N. *Constr. Build. Mater.* **2013**, *41*, 545.
20. Matuana, L. M.; Woodhams, R. T.; Balatinecz, J. J.; Park, C. B. *Polym. Compos.* **1998**, *19*, 446.
21. Matuana, L. M.; Balatinecz, J. J.; Park, C. B. *Polym. Eng. Sci.* **1998**, *38*, 1862.
22. Matuana, L. M.; Balatinecz, J. J.; Park, C. B.; Woodhams, R. T. *Wood Fiber. Sci.* **1999**, *31*, 116.
23. Martinez-Camacho, A. P.; Cortez-Rocha, M. O.; Ezquera-Brauer, J. M.; Graciano-Verdugo, A. Z.; Rodriguez-Felix, F.; Castillo-Ortega, M. M.; Yepiz-Gomez, M. S.; Plascencia-Jatomea, M. *Carbohydr. Polym.* **2010**, *82*, 305.
24. Ou, C. Y.; Zhang, C. H.; Li, S. D.; Yang, L.; Dong, J. J.; Mo, X. L.; Zeng, M. T. *Carbohydr. Polym.* **2010**, *82*, 1284.
25. No, H. K.; Park, N. Y.; Lee, S. H.; Meyers, S. P. *Int. J. Food Microbiol.* **2002**, *74*, 65.
26. Liu, X. F.; Guan, Y. L.; Yang, D. Z.; Li, Z.; Yao, K. D. *J. Appl. Polym. Sci.* **2001**, *79*, 1324.
27. Faisal, A.; Salmah, H.; Kamarudin, H. *Compos. A* **2013**, *46*, 89.
28. Salmah, H.; Faisal, A.; Kamarudin, H. *Int. J. Polym. Mater.* **2011**, *60*, 429.
29. Salmah, H.; Faisal, A.; Kamarudin, H.; Hanafi, I. *J. Vinyl Addit. Technol.* **2011**, *17*, 125.
30. Salmah, H.; Faisal, A.; Kamarudin, H. *Polym. Plast. Technol.* **2012**, *51*, 86.
31. Shah, B. L.; Matuana, L. M. *J. Vinyl Addit. Technol.* **2005**, *11*, 160.
32. Xu, K. M.; Li, K. F.; Zhong, T. H.; Guan, L. T.; Xie, C. P.; Li, S. *Compos. B* (Submitted).
33. Shi, L.; Zhao, Y.; Zhang, X. D.; Su, H. J.; Tan, T. W. *Korean J. Chem. Eng.* **2008**, *25*, 1434.
34. Shahidi, F.; Arachchi, J. K. V.; Jeon, Y. J. *Trends Food Sci. Tech.* **1999**, *10*, 37.
35. Niu, M.; Liu, X. G.; Dai, J. M.; Jia, H. S.; Wei, L. Q.; Xu, B. S. *Carbohydr. Polym.* **2009**, *78*, 54.
36. Sanpui, P.; Murugadoss, A.; Durga Prasad, P. V.; Ghosh, S. S.; Chattopadhyay, A. *Int. J. Food Microbiol.* **2008**, *124*, 142.
37. Mohan, T. P.; Kanny, K. *Compos. A* **2011**, *42*, 385.
38. Reddy, C. R.; Sardashti, A. P.; Simon, L. C. *Compos. Sci. Technol.* **2010**, *70*, 1674.
39. Zhang, H. Z.; He, Z. C.; Liu, G. H.; Qiao, Y. Z. *J. Appl. Polym. Sci.* **2009**, *113*, 2018.
40. Theodorou, M.; Jasse, B. *J. Polym. Sci. Polym. Phys.* **1983**, *21*, 2263.
41. Dash, B. N.; Rana, A. K.; Mishra, H. K.; Nayak, S. K.; Mishra, S. C.; Tripathy, S. S. *Polym. Compos.* **1999**, *20*, 62.
42. Felix, J. M.; Gatenholm, P. *J. Appl. Polym. Sci.* **1991**, *42*, 609.
43. Mohanty, S.; Nayak, S. K. *J. Appl. Polym. Sci.* **2006**, *102*, 3306.
44. Dhakal, H. N.; Zhang, Z. Y.; Richardson, M. O. W. *Compos. Sci. Technol.* **2007**, *67*, 1674.
45. Kim, H. J.; Seo, D. W. *Int. J. Fatigue* **2006**, *28*, 1307.